ELSEVIER

Polymer 42 (2001) 9261–9268

polymer

www.elsevier.com/locate/polymer

Association behavior of poly(*N*,*N*-dimethylacrylamide)-*graft*-poly (methyl methacrylate) in dilute solution

M. Itakura, K. Inomata[1], T. Nose*

Department of Polymer Chemistry and International Research Center of Macromolecular Science, Tokyo Institute of Technology, O-okayama, Meguro-ku, Tokyo 152-8552, Japan

Received 29 January 2001; received in revised form 7 June 2001; accepted 18 June 2001

Abstract

Association behavior of poly(*N*,*N*-dimethylacrylamide)-*graft*-poly(methyl methacrylate) in dilute solution of mixed solvent of methanol/water has been investigated by using light scattering, where association strength of grafted chains is controlled by changing the water content. The following points are demonstrated: (1) the increase in water content in solvent starting from pure methanol increases the association strength, resulting in the formation of inter-molecular associations at water contents higher than 20–30 wt% of water, (2) the association number, N_a, depends on the changing rate of water content of solvent. At higher changing rates, associates of small N_a (= 2–4) are formed by the dominance of intra-molecular association, while the slower change of water content yields larger associates of N_a being of the order of 10. The presence of the optimum changing rate of solvent quality for inter-molecular associations is suggested. This process dependence of associate structure is discussed on the basis of association kinetics.

Keywords: Graft copolymer; Association behavior; Intra-molecular association

1. Introduction

Micellization behavior of di- and tri-block copolymers in selective solvent has been extensively studied both experimentally and theoretically. In these cases, the micelle is formed by many-chain associations because single chains have only one or two associative chain segments. On the contrary, graft copolymers having many associative side chains can form micelles with less number of molecules, even unimolecular micelles by intra-molecular association. Furthermore, combination of intra- and inter-molecular association leads to diverse possible structures of associates. In spite of being an attractive research subject, very few studies on it have been reported [1–15]. Kikuchi and Nose [13–15] have extensively studied structures of graft-copolymer micelles in selective solvent as functions of solvent quality, grafted-chain density, and polymer concentration using poly(methyl methacrylate)-*graft*-polystyrene, and found string-slower type unimolecular micelles and their inter-molecular associates of semi-flexible rods. This unimolecular structure has theoretically been predicted by Halperin [16] and de Gennes [17]. Tanaka and Koga [18] have studied, by computer simulations, intra- and inter-molecular associates of polymer molecules having many associative units in a chain.

In this paper, we study the association behavior of poly(*N*,*N*-dimethylacrylamide)-*graft*-poly(methyl methacrylate) (PDMA-*g*-PMMA) in dilute solution of mixed solvent of methanol/water by means of light scattering. Increasing the water content of methanol/water solvent, we can make the solvent quality become worse for grafted PMMA chains, which induces associations of the grafted chains. The structure of associates is found to dramatically change with the rate of solvent-quality change. In the following sections, we will report on the preparation of the graft copolymer, preparation processes of sample solutions, and present the results of light scattering measurements with their analyses. The association number and the structure of associates estimated from the experimental results will be discussed as functions of solvent quality, polymer concentration, and the rate of solvent-quality change.

* Corresponding author. Present address: Department of Applied Chemistry, Tokyo Institute of Polytechnics, 1583 Iiyama, Atsugi-shi, Kanagawa 243-0297, Japan. Tel./fax: +81-46-242-9524.

E-mail address: nose@chem.t-kougei.ac.jp (T. Nose).

[1] Present address: Department of Materials Science and Engineering, Nagoya Institute of Technology, Gokiso-cho, Showa-ku, Nagoya 466-8555, Japan.

0032-3861/01/$ - see front matter
PII: S0032-3861(01)00463-3

2. Experiments

2.1. Materials

PDMA-*g*-PMMA was prepared by radical copolymerization of *N*,*N*-dimethylacrylamide (DMA) and PMMA macromonomer (vinyl-PMMA) with 2,2′-azobis(isobutyronitrile) (AIBN) as initiator. Vinyl-PMMA, having a styrene group at one terminal, was purchased from Polymer Source, Inc., and used as received. DMA was fractionally distilled just before polymerization. AIBN was recrystallized from methanol solution. The copolymerization was carried out at 53°C in dioxane, which was purified by drying on calcium hydride, followed by fractional distillation. The total monomer concentration was 50 wt% of solution with vinyl-PMMA and AIBN being, respectively, of 5 wt% and 1/20 000 in mole for the total monomers. The conversion was controlled to be 30 wt% to reduce the composition distribution width of copolymers. The solution after stopping the polymerization was diluted by chloroform, followed by precipitation with hexane to make fractionation by molecular weight, and obtain samples with narrow distributions of molecular weight. In Table 1 are listed the characteristics of fractionated PDMA-*g*-PMMA used in this study, which have been measured by using light scattering, size exclusion chromatography, and ^{1}H nuclear magnetic resonance spectroscopy.

Methanol (MeOH), water, and tetrahydrofurane (THF) were used as solvents in light scattering measurements. MeOH and THF were dried on calcium oxide and on calcium hydride, respectively, and then fractionally distilled. Water used was purified by Milli-Q Jr (Millipore Co.).

2.2. Preparation of sample solutions

PDMA-*g*-PMMA is molecularly dissolved in MeOH, and forms associates with cores of grafted PMMA in MeOH/water mixed solvent containing water more than a certain amount. Preparation of sample solution was performed in the following way: We always start with dissolving the copolymer in pure MeOH molecularly, and then added water by different adding processes. PDMA-*g*-PMMA/MeOH solution was mildly stirred overnight, and optically purified through Millipore filters of nominal pore size of 0.2 μm before use. The water-adding processes were of the following three types: (1) starting with MeOH solutions of various polymer concentrations, we added water so as to increase water content by about 8% in every 120 min, i.e. we waited for 60 min to equilibrate the solution and measured light scattering for 1 h, and then added water to go to the next solvent composition. (2) Starting with 0.2 wt% MeOH solution, we took a process similar to process (1), but changed water content by 8% with various time intervals (t_{interval}). (3) To attain the quickest water addition, we added water at a time to make the solution of 50 wt% water content. Processes (1) and (3) can be referred to as the processes of $t_{\text{interval}} = 120$ and 0 min, respectively.

Table 1
Characteristics of PDMA-*g*-PMMA

Total M_w [a]	9.0×10^5 g/mol
M_w/M_n [b]	1.13
Weight fraction of side chains [c]	9.3 wt%
M_w of main chain	8.2×10^5 g/mol
M_w of side chain	5.0×10^3 g/mol
Averaged number of side chains in a molecule	16.7

[a] Static light scattering for THF solution.
[b] Size exclusion chromatography using *N*,*N*-dimethylformamide (contains 0.1 mol% lithium bromide) as eluent and standard polystyrene for calibration.
[c] ^{1}H nuclear magnetic resonance spectroscopy for chloroform-d_1 solution.

2.3. Light scattering measurements

The light scattering apparatus was a laboratory-made one using an Ar ion laser operating at the wavelength of 488 nm as light source and SO-SIPD/DUAL as detector connecting with an ALV-5000 correlator. The details of the equipment has been described elsewhere [19]. To characterize the PDMA-*g*-PMMA samples, we made a conventional static light scattering analysis of the Zimm plots using the following equation in terms of the excess Rayleigh ratio $R_{VV}(q)$, weight-average molar mass M_w, the radius of gyration R_g, and the second virial coefficient A_2.

$$\frac{KC}{R_{VV}(q)} = \frac{1}{M_w}\left[1 + \frac{R_g^2}{3}q^2 + \cdots\right] + 2A_2C + \cdots \qquad (1)$$

where K is the optical constant defined by $K = 4\pi^2 n^2 (\partial n/\partial C)^2/(N_A\lambda_0^4)$ with n, $(\partial n/\partial C)$ λ_0 and N_A being refractive index, the refractive index increment, the wave length of incident beam, and the Avogadro constant, respectively. The wave number q is given by $q = (4\pi n/\lambda_0)\sin(\theta/2)$ in terms of scattering angle θ, and the polymer concentration C has the unit of g/ml. The refractive index increments were measured to be 0.144 ml/g in MeOH and 0.076 ml/g in THF. The values of refractive indices for MeOH and water are so close to each other that the composition dependence was ignored for the refractive index increment of the MeOH/water mixed solvent. The copolymer used here, PDMA-*g*-PMMA, which must have some composition distribution, is optically regarded as a homopolymer [20] because the refractive index increments for PDMA and PMMA chains are relatively close to each other, and the PMMA fraction is small. In light scattering analyses for associating polymer solutions, the A_2 term was ignored since the concentration was reasonably dilute and the extrapolation to the dilute limit may not be allowed because of the change in association behavior with the concentration. The values obtained with no extrapolation are here referred to as apparent values indicated by the subscript 'app'.

Furthermore, associates have large particle sizes, so that the particle scattering function with no expansion with respect to q will be used, of which details will be presented later.

Time-correlation functions of scattered light intensity were converted to the correlation function of electric field on the basis of the homodyne scattering. Then, the distribution of decay rate was obtained by the CONTIN analysis. The distributions obtained had single peaks, of which position gave average decay rates Γ. The decay rate was transformed to the diffusion coefficient D by $\Gamma = Dq^2$, and then to the hydrodynamic radius R_h by using the Einstein–Stokes equation:

$$R_h = \frac{k_B T}{6\pi\eta D} \tag{2}$$

where k_B, T, and η are the Boltzmann constant, the absolute temperature, and solvent viscosity, respectively. Here again, as in the analyses of static light scattering, no dilute-limit extrapolation was available, hence the obtained values were apparent in this sense. All the measurements were carried out at 20.0°C, which was controlled within ±0.01°C.

3. Results and discussion

3.1. Dependencies on solvent composition of MeOH/water

Fig. 1 shows the Zimm-type plots, i.e. the inverse of scattered light intensities I multiplied by the concentration C plotted against $\sin^2(\theta/2)$, for the sample prepared by process (1) of the starting polymer concentration being 0.2 wt% described in Section 2. The intensity sharply increases around the solvent composition of 20–50 wt% water content, suggesting a change from non-associating unimer region to associating region. In the respective limiting regions, the plots are almost falling on straight lines, while in the crossover region, the plots are making bended

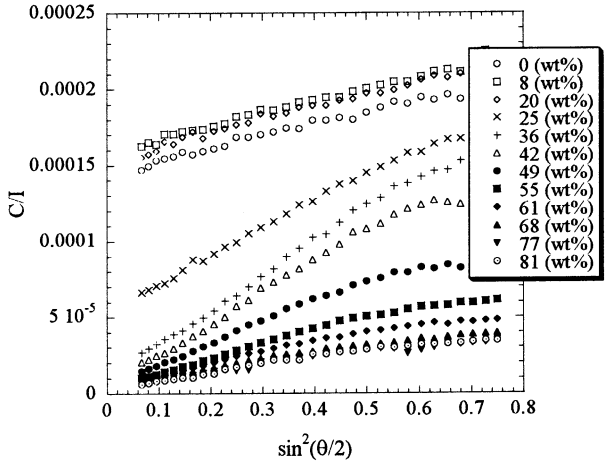

Fig. 1. Zimm-type plots of scattered light intensity of PDMA-*g*-PMMA in MeOH/water mixed solvents of various water contents prepared by diluting 0.2 wt% MeOH solution with water.

curves, suggesting bi-modal or wide particle size distributions. In Fig. 2 are shown the decay-rate distribution functions obtained from dynamic light scattering at $\theta = 30°$ for the same sample as a function of the water content of solvent. At small water contents, the distribution exhibits a sharp single peak at higher decay rates, and then having another peak at lower decay rates to become bi-modal as the water content increases. At the same time, the fast mode peak shifts towards smaller decay rate a little primarily owing to the increase in solvent viscosity. With further increase in the water content, the decay-rate distribution having the fast and slow mode peaks exhibit no essential change with water content, although it seems to become slightly broader. These findings indicate the change from non-associating to formation of associates. There are observed three regions in principle, the unimer, the transitional, and the associating regions both static and dynamic light scatterings.

3.2. Bimodal analyses of light scattering data

Static and dynamic light scattering show bimodal behavior, in particular, in the transitional region of the water content of mixed solvent ranging from 20 to 50 wt%. To analyze the static bimodal data, we use [21]

$$\frac{KC}{R(q)} = \left[A^{\text{small}}(q) + A^{\text{large}}(q)\right]^{-1} \tag{3}$$

under the approximation of dilute limit. Here, $A(q)$ is the product of wM and the particle scattering function $P(q)$, with w and M being the weight fraction of smaller or larger particles of molecular weight M. The amplitude of $A(0) = A^{\text{small}}(0) + A^{\text{large}}(0)$ corresponds to M_{wapp}. For the fast mode of smaller particles, qR_g is smaller than unity, so that the particle scattering function can be expressed as

$$P(q) = 1 - \frac{1}{3}R_g^2 q^2 + \cdots \tag{4}$$

For the slow mode of larger particles, we tried to fit $P(q)$s of various shapes to the data in the associating region, and obtained the best fittings by $P(q)$ of a cylindrical shape. That is, we used the following particle scattering function for a cylinder of the radius R and the length L in terms of $X_R = qR$ and $X_L = qL/2$ [22].

$$P(q) = \int_0^{\pi/2} \frac{\sin^2(X_L \cos\beta)}{X_L^2 \cos^2\beta} \frac{4J_1^2(X_R \sin\beta)}{X_R^2 \sin^2\beta} \sin\beta \, d\beta \tag{5}$$

where $J_1(x)$ is the first order Bessel function. The radius of gyration is given by

$$R_g^2 = R^2/2 + L^2/12 \tag{6}$$

Furthermore, we used the fixed value of $L/2R = 5$ since this value gave the best fit, although the data fittings could not determine more precise values of $L/2R$ by taking it as adjustable parameter in fitting. Since the decay-rate distribution functions obtained from dynamic light scattering

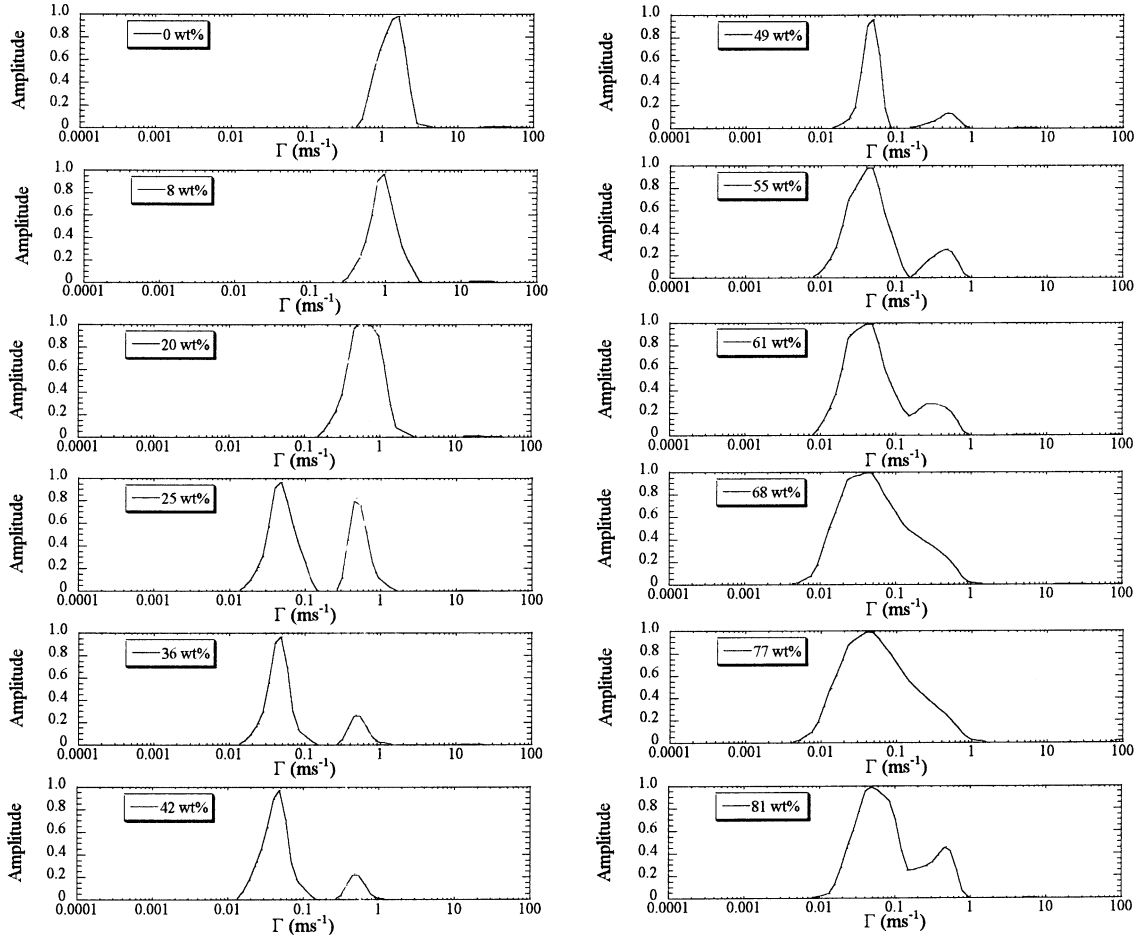

Fig. 2. Decay-rate distributions of dynamic light scattering at $\theta = 30°$ for PDMA-*g*-PMMA in MeOH/water mixed solvents of various water contents prepared by diluting 0.2 wt% MeOH solution with water.

exhibit sharp peaks for two respective modes, the polydispersity of particle size can reasonably be neglected, although the neglect may give some inaccuracy to quantitative results of the analysis. The fitting can evaluate M_{wapp}, R_{gapp} for both components, and the amplitude ratio $A_m = A^{large}(0)/A(0)$. Fig. 3 illustrates an example of the fittings. Dynamic data analyzed by the CONTIN program give the hydrodynamic radii R_{happ} and the amplitude ratios.

All these quantities, M_{wapp}, $A^{large}(0)/A(0)$, R_{gapp}, and R_{happ}, obtained by static and dynamic light scattering, are summarized as functions of the water content of mixed solvent in Fig. 4(a)–(d), respectively. The size of associates is almost constant irrespective of the solvent quality once the associates start to form. Therefore, in the transitional region, the increase in the fraction of associates dominates over the growth of associate size. The associates formed by process (1) with $t_{interval} = 120$ min have the association number of the order of 100 or a little smaller with the particle size being a couple of 100 nm.

3.3. Dependencies on polymer concentration

The polymer concentration is not constant during the

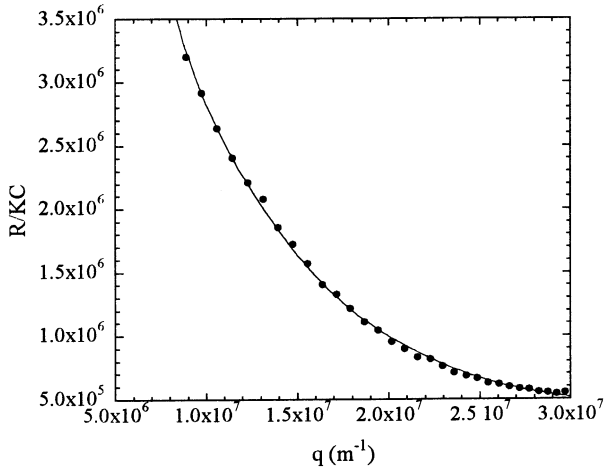

Fig. 3. An example of bimodal fittings (solid line) for experimental angular dependence of scattered light intensity (circles). (See the text for the details of the analysis.) The fitting was carried out with $L/2R = 5$ for the solution of $t_{interval} = 120$ min with the polymer concentration of 1.39×10^{-3} (g/g) in MeOH/water mixed solvent with the water content of 36 wt%.

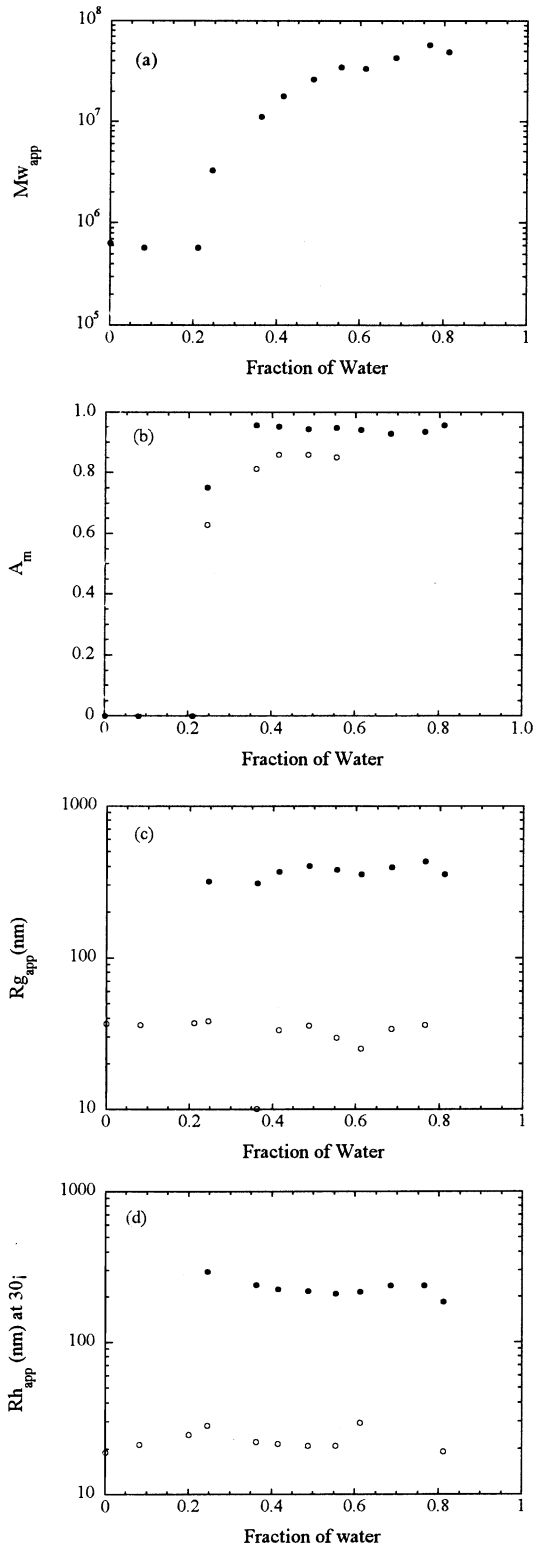

Fig. 4. M_{wapp}, A_m ($= A^{large}(0)/A(0)$), R_{gapp}, and R_{happ} as functions of the water content of MeOH/water mixed solvent obtained from static and dynamic light scattering for PDMA-*g*-PMMA solutions prepared by diluting 0.2 wt% MeOH solution. (a) M_{wapp}, (b) A_m from static (solid circles) and dynamic (hollow circles) light scattering, (c) R_{gapp} and (d) R_{happ} for small particles (unimers) (hollow circles) and large particles (aggregates) (solid circles).

sample preparation processes (1)–(3), but becomes more dilute with the addition of water. For instance, if we start with the 0.2 wt% solution, then the polymer concentration of the solution at 50 wt% water content is 0.1 wt%. To see the polymer concentration effects on the association behavior, we performed the same experiments for the solutions prepared by process (1) with different starting concentrations ranging from 0.1 to 0.5 wt%. The experimental observations demonstrate that there is nothing different in association behavior for the solutions of different concentrations, but the solvent composition at the onset of association slightly shifts towards the less water content. That is, the onset water content changes from 40 to 20 wt% for the starting polymer concentration changing from 0.1 to 0.5 wt%. This implies that higher concentration needs less association strength, which is quite reasonable.

3.4. Effects of changing rate of solvent quality

Fig. 5 shows the Zimm-type plots of scattered light intensity in semi-log scale for solutions with different time intervals $t_{interval}$ ranging 0–180 min, along with those for MeOH solution as reference. It is noted that the intensities presented here are those observed when the intensity became stationary after about a few 10% increase of the intensity at the final water content of 50 wt%. Usually, it took half a day or a day for the stabilization of intensity after the water content reached 50 wt%. Fig. 5 obviously shows a strong dependence of the static light scattering on the preparation process, i.e. $t_{interval}$, demonstrating that the structure of associates formed is controlled by the rate of solvent quality change. In Fig. 6, the decay-rate distributions are illustrated for different $t_{interval}$ corresponding to the static light scattering shown in Fig. 5. Figs. 5 and 6 indicate that the rapid change of solvent quality, $t_{interval} < 60$ min, leads small association numbers with unimodal particle size

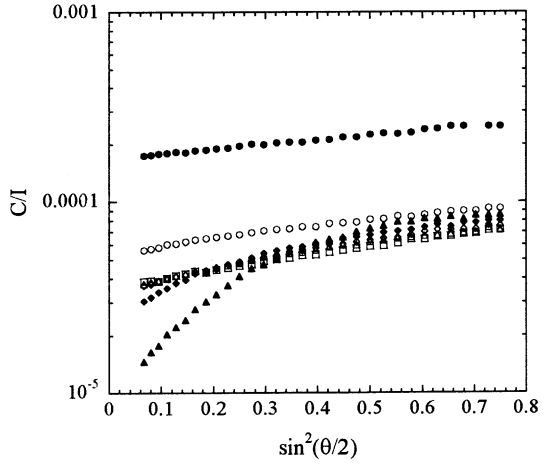

Fig. 5. Zimm-type plots of scattered light intensity for 0.1 wt% PDMA-*g*-PMMA in MeOH/water mixed solvent with the water content of 51 wt% with various interval times, $t_{interval}$. $t_{interval} = 0$ min (○), 10 min (□), 30 min (◇), 60 min (△), 120 min (▲), and 18 min (◆). (●) 0.1 wt% MeOH solution.

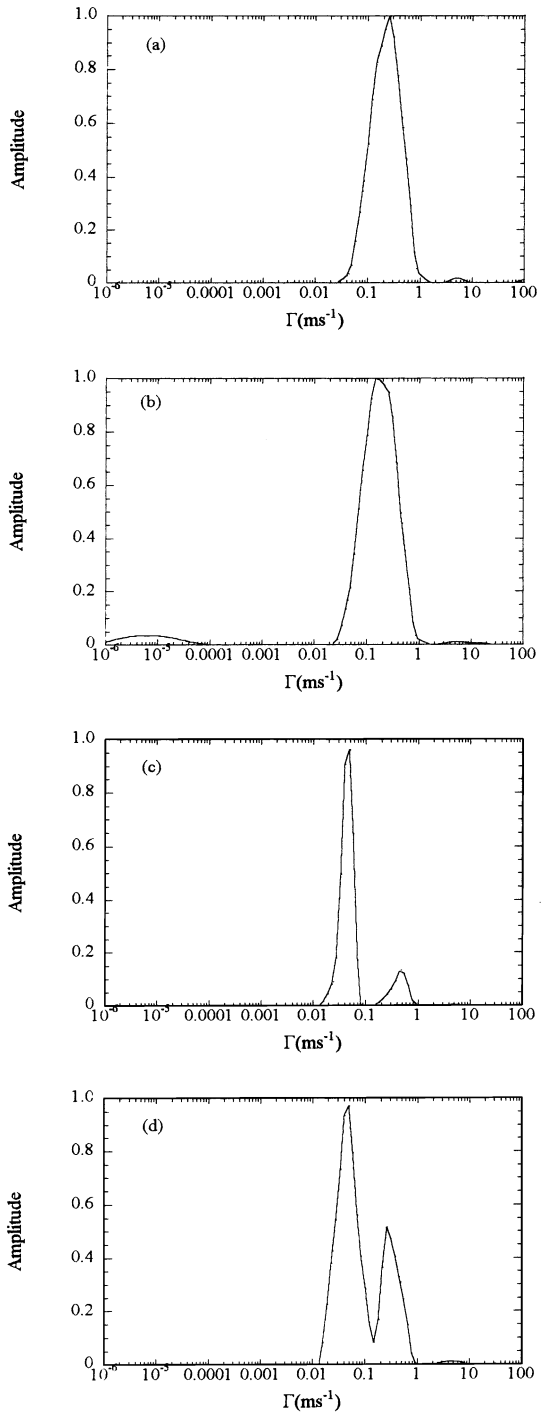

Fig. 6. Decay-rate distributions of dynamic light scattering at $\theta = 30°$ for 0.1 wt% PDMA-*g*-PMMA in MeOH/water mixed solvents with the water content of 51 wt% prepared with different interval times, $t_{interval}$. (a) $t_{interval} = 0$ min, (b) 60 min, (c) 120 min, and (d) 180 min.

distributions, while the slower change, $t_{interval} > 120$ min, induces the large associates with bimodal distributions. Using the same analyses as those adopted in Section 3.3, we list more quantitative results in Table 2. In Table 2, the results for 0.1 wt% MeOH and THF solutions, and that for THF solution after the extrapolation to $C = 0$ according to Eq. (1) are also listed as reference. When $t_{interval} < 60$ min, the association number, N_a is small, 2–4, and N_a is about 10 at $t_{interval} = 180$ min. At $t_{interval} = 120$ min, N_a is the largest, around 40, suggesting the presence of the optimum rate of solvent quality change for inter-molecular associations. At faster rates, at $t_{interval} < 60$ min, the solvent quality changes to be bad enough to PMMA chains faster than the inter-molecular association rate, so that the inter-molecular associations dominating over the inter-molecular bonding make the copolymer chains more stable for further inter-molecular associations by consuming free associative grafted chains. At slower rates, $t_{interval} > 120$ min, the solvent quality changes to become gradually worse to grafted chains, so that both intra- and inter-molecular associations can take place to induce formation of inter-molecular association appreciably. If the rate of solvent quality change is so slow, associates formed at marginally bad solvent quality become rather stable by association rearrangements before the solvent quality changes to be very bad to PMMA chains. Therefore, there seems to be the optimum rate of solvent quality change for inter-molecular associations, where the structure formed at the marginal solvent quality is not so stable and the further decrease in solvent quality induces more inter-molecular associations leading to further associations. The change of solvent quality from poor to bad takes place rather in a narrow range of MeOH/water composition, around 20–30 wt% water contents. The rate of solvent quality change around that range of water content may primarily control the association number by balancing intra- and inter-molecular associations.

3.5. Structure of associates

In good solvent (THF)to both PDMA and PMMA, the copolymer exhibits random coils having R_g/R_h ratio (see Table 2) similar to those of linear homopolymers. In pure MeOH, which is a weakly selective solvent to PDMA, the chain radius is a little larger than that in the good solvent, and the ratio of R_g/R_h is much larger than that for the spherical globule, even a little larger than those for swollen random coil chains. This may imply an elongated or stretched shape owing to an imperfect association. The same feature has been observed for poly(methyl methacrylate)-*graft*-polystyrene under a similar condition [13].

Associates having small association numbers, N_a, formed the quick change of the solvent quality and have a radii of about 50 nm with the ratio of R_g/R_h being around unity, as shown in Table 2. Considering molecular masses of the associates and the molar mass M_s (~50 000 g/mol) of the average segmental main chain size between neighboring graft points, these findings suggest that the structure of associates may be of the flower-type globule.

Inter-molecular associates of N_a being of the order of several tens formed at $t_{interval} \geq 120$ min must take shrunken globular shape, reasonably having the size of a few 100 nm and the R_g/R_h of about 1.5. As mentioned in Section

Table 2
Results of light scattering analyses for interval-time dependency

$t_{interval}$ (min)	Fraction of water	M_{wapp}	R_{gapp} (nm)	R_{happ} (nm)	R_g/R_h
0	0.51	1.5×10^6	44	43	1.0
10	0.51	2.4×10^6	59	59	1.0
30	0.52	2.4×10^6	63	64	1.0
60	0.51	2.4×10^6	62	61	1.0
120	0.49	2.7×10^7			
		$A_m = 0.94$	402	218	1.8
		$A_u = 0.06$[a]	36	21	1.7
180	0.51	7.7×10^6			
		$A_m = 0.82$	322	209	1.5
		$A_u = 0.18$	32	29	1.1
0.1 wt% MeOH solution		5.6×10^5	43	22	1.9
0.1 wt% THF solution		6.8×10^5	30	18	1.7
THF solution, dilute limit[b]		9.0×10^5	33	19	1.7

[a] A_u denotes the fraction of small aggregates expressed by the scattering amplitude, i.e. $A_u = A^{small}(0)/A(0)$.
[b] Result after the extrapolation to $C = 0$ according to Eq. (1). Therefore, the values of M_w, R_g, and R_h are not apparent ones.

3.4, the particle scattering function $P(q)$ for data fittings suggests the cylindrical shape of the length-to-radius ratio, $L/2R$, being about 5, which implies $L \sim 1400$ nm, and $R \sim 135$ nm for $R_g \sim 400$ nm, for example. The obtained value of radius R of elongated associates is larger than the fully extended loop length (~40 nm) estimated from the average molar mass M_s between neighboring grafted points even added the length (~8 nm) of a fully extended PMMA chain forming association cores. This may suggest a wide distribution of M_s and a loose structure of the core part of associate, which may not be a single core of tightly bonded chains, but consist of many cores concentrated in central part of the whole associate.

4. Conclusions

Association behavior of PDMA-*g*-PMMA with low graft number density but many branches in a chain has been investigated using light scattering. By changing the association strength with the increase in the water content of MeOH/water mixed solvent, we observe association behavior depending on intra- and inter-molecular associations of grafted chains. The following points are demonstrated:

1. The increase in water content increases the association strength of grafted chains, leading to the formation of inter-molecular association at higher water contents above 20–330 wt% of water.
2. The association number, N_a, dramatically depends on the changing rates of water content of solvent. At higher changing rates, associates of less N_a (= 2–4) are formed by the dominance of intra-molecular associations, while the slower change in water content yields larger associates of N_a being of the order of several 10s. There seems to be the optimum changing rate of solvent quality for inter-molecular associations. These process dependencies of formed associates can be understood by using association kinetics.
3. The associates of larger N_as are estimated to have an elongated globular shape.

Acknowledgements

This work was partly supported by a Grant in Aid for Scientific Research (no. 10305066) from the Ministry of Education, Science, Sports and Culture of Japan.

References

[1] Pitsikalis M, Woodward J, Mays JW, Hadjichristidis N. Macromolecules 1997;30(18):5384–9.
[2] Price C, Woods D. Polymer 1973;14:82–6.
[3] Price C, Woods D. Polymer 1974;15:389–92.
[4] Kotaka T, Tanaka T, Inagaki H. Polym J 1972;3:327–37.
[5] Kotaka T, Tanaka T, Inagaki H. Polym J 1972;3:338–49.
[6] Selb J, Gallot Y. Makromol Chem 1981;182:1775–86.
[7] Tuzar Z, Kratochvil P, Prochazka K, Contractor K, Hadjichristidis N. Makromol Chem 1989;190:2967–73.
[8] Ma Y, Cao T, Webber WE. Macromolecules 1998;31(6):1773–8.
[9] Bronich TK, Cherry T, Vinogradov SV, Eisenberg A, Kabanov VA, Kabanov AV. Langmuir 1998;14:6101–6.
[10] Hashizume A, Mizusaki M, Yoda K, Morishima Y. Langmuir 1999;15(12):4276–82.
[11] Morishima Y, Nomura S, Ikeda T, Seki M, Kamachi M. Macromolecules 1995;28(8):2874–81.
[12] Yamamoto H, Mizusaki M, Yoda K, Morishima Y. Macromolecules 1998;31(11):3588–94.
[13] Kikuchi A, Nose T. Macromolecules 1996;29(21):6770–7.
[14] Kikuchi A, Nose T. Macromolecules 1997;30(4):896–902.
[15] Kikuchi A, Nose T. Polymer 1996;37(26):5889–96.

[16] Halperin A. Macromolecules 1991;24(6):1418–9.
[17] de Gennes PG. Isr J Chem 1995;35:33–5.
[18] Tanaka F, Koga T. Comp Theoret Polym Sci 2000;10:259–67.
[19] Varma B, Fujita Y, Takahashi M, Nose T. J Polym Sci, Polym Phys Ed 1984;22:1781–97.
[20] Benoit H, Floelich D. In: Huglin MB, editor. Light scattering from polymer solutions. New York: Academic Press, 1972, Chapter 11.
[21] Fukumine Y, Inomata K, Takano A, Nose T. Polymer 2000;41:5367–74.
[22] Burchard W. Adv Polym Sci 1983;48:1.